Characterisation and evaluation of a new phase change enhanced working solution for liquid desiccant cooling systems

Haoshan Ren
University of Wollongong, hr681@uowmail.edu.au

Zhenjun Ma
University of Wollongong, zhenjun@uow.edu.au

Stefan Gschwander
Fraunhofer Institute for Solar Energy Systems ISE

Characterisation and evaluation of a new phase change enhanced working solution for liquid desiccant cooling systems

Abstract

Desiccant solutions play an essential role in desiccant cooling systems to absorb moisture from the process air. This paper presents the characterisation of a new working solution for liquid desiccant cooling systems. The new working solution was prepared through dispersion of micro-encapsulated phase change materials (MPCMs) into lithium chloride (LiCl) desiccant solutions to ensure that the dehumidification process was achieved under a low temperature condition and to improve thermal capacity and moisture removal efficiency of the mixture. The properties of the new solution, including density, enthalpy-temperature relationship, particle size distribution, thermal conductivity, and vapour pressure were characterised through either experimental tests or theoretical analysis. It was shown that the density and thermal conductivity of the new working solution slightly decreased with the increase of the mass fraction of the MPCMs in the mixture. The thermal capacity of the new working solution substantially increased in the melting temperature range of the MPCMs used. The vapour pressure of the new working solution decreased due to the existence of the MPCM particles. It is expected that the dehumidification efficiency of adiabatic dehumidifiers can be potentially improved when using this new working solution due to the decreased vapour pressure and increased thermal capacity of the phase change enhanced desiccant solution.

Disciplines

Engineering | Science and Technology Studies

Publication Details

1 # Characterisation and evaluation of a new phase change enhanced

2 # working solution for liquid desiccant cooling systems

3 Haoshan Ren[1], Zhenjun Ma[1,*], Stefan Gschwander[2]

4 [1]Sustainable Buildings Research Centre, University of Wollongong, 2522, Australia

5 [2]Fraunhofer Institute for Solar Energy Systems, Freiburg, 79110, Germany

6 *Email: zhenjun@uow.edu.au

7

8 **Abstract**: Desiccant solutions play an essential role in desiccant cooling systems to absorb

9 moisture from the process air. This paper presents the characterisation of a new working

10 solution for liquid desiccant cooling systems. The new working solution was prepared through

11 dispersion of micro-encapsulated phase change materials (MPCMs) into lithium chloride (LiCl)

12 desiccant solutions to ensure that the dehumidification process was achieved under a low

13 temperature condition and to improve thermal capacity and moisture removal efficiency of the

14 mixture. The properties of the new solution, including density, enthalpy-temperature

15 relationship, particle size distribution, thermal conductivity, and vapour pressure were

16 characterised through either experimental tests or theoretical analysis. It was shown that the

17 density and thermal conductivity of the new working solution slightly decreased with the

18 increase of the mass fraction of the MPCMs in the mixture. The thermal capacity of the new

19 working solution substantially increased in the melting temperature range of the MPCMs used.

20 The vapour pressure of the new working solution decreased due to the existence of the MPCM

21 particles. It is expected that the dehumidification efficiency of adiabatic dehumidifiers can be

22   potentially improved when using this new working solution due to the decreased vapour

23   pressure and increased thermal capacity of the PCM-LiCl desiccant solution.

24   **Keywords**: Desiccant cooling; phase change material; new working solution; characterisation;

25   vapour pressure.

26

27   **Nomenclature**

28   d diameter (m)

29   h enthalpy (J/kg)

30   k thermal conductivity (W/m K)

31   m mass (kg)

32   P vapour pressure (Pa)

33   t time (s)

34   T temperature (ºC)

35   x_m mass fraction

36   x_v volume fraction

37

38   *Greek symbols*

39   α coefficient

40   α_R equivalent thermal conductivity depression

41   β coefficient

42   θ reduced temperature

| 43 | π | coefficient |
| 44 | ρ | density (kg/m^3) |

45

46 *Subscripts*

47	*a*	air
48	*c*	core
49	*e*	equivalent
50	*LiCl*	lithium chloride desiccant solution
51	*PCM*	micro-encapsulated phase change material
52	*PCM-LiCl*	phase change enhanced LiCl desiccant solution
53	*s*	shell

54

1. Introduction

56   Air conditioning is essential to our lives and is greatly impacting the quality of our life and

57   even saves lives during intense heat waves [1]. The amount of installed air conditioning systems

58   is expected to increase dramatically in the coming decades, largely driven by economic growth

59   and global warming [2]. Nowadays, the majority of air conditioning systems used were

60   developed based on the vapour compression cycle [3]. These systems can control sensible load

61   effectively but are very inefficient to deal with latent load, in particular under hot and humid

62   climatic conditions. This is because a significant amount of energy is required to dehumidify

63   the air by overcooling the air below its dew point temperature in order to remove the moisture

64   through condensation and then heating it to the desired temperature [4].

65   Liquid desiccant cooling as one of the alternative solutions has received increasing attention

66   for air conditioning and dehumidification due to its effectiveness in humidity control and great

67   potentials in energy savings [5-7]. A liquid desiccant is generally a concentrated salt solution

68   such as lithium bromide (LiBr), lithium chloride (LiCl), and calcium chloride (CaCl$_2$) that

69   directly absorbs moisture without cooling the air below its dew point. Liquid desiccant cooling

70   can be driven by low-grade thermal energy (50-90 ºC) such as waste heat or solar energy [8].

71   As the building peak cooling demand generally occurs at approximately the same time as local

72   peak solar radiation, this opens up opportunities of using solar energy to drive liquid desiccant

73   cooling and even to take air conditioning off the grid with the assistance of thermal energy

74   storage systems.

75   Various types of liquid desiccant cooling systems and their potentials to maintain

76   acceptable indoor thermal comfort under different climatic conditions have been studied. Ham

77   et al. [9], for instance, developed a liquid desiccant and dew point evaporative cooling assisted

78   100% outdoor air system. The simulation results showed that 12% of the primary energy can

79   be saved by using this system, in comparison with a typical variable air volume system. Elmer

80   et al. [10] developed a liquid desiccant cooling system consisting of a regenerator, a

81   dehumidifier and an evaporative inter-cooler integrated with an energy exchanger. The

82   experimental results showed that the dehumidification effectiveness of this system was 30-47%

83   with an average electrical COP of 2.5. Chen et al. [11] proposed a liquid desiccant dehumidifier

84   and a regenerative indirect evaporative cooling system for fresh air treatment. The thermal

85　energy obtained from solar collectors was used for liquid desiccant regeneration. The results

86　showed that the energy saving of this system was 22.4-53.2% under various inlet air conditions,

87　in comparison to a conventional chilled water air conditioning system. A solar driven liquid

88　desiccant cooling system was developed by a company named L-DCS Technology [12]. This

89　system was installed in a building in Singapore and used for cooling and dehumidification [13].

90　　A dehumidifier is a key component in a liquid desiccant cooling system. Adiabatic

91　dehumidifiers are relatively simple units, but they must work with a high desiccant flow rate

92　and a high air flow rate in order to achieve a better dehumidification efficiency [6, 14]. In

93　adiabatic dehumidifiers, the temperature of the desiccant solution continuously increases along

94　the desiccant flow direction. The increase in the solution temperature deteriorates the

95　dehumidification efficiency as the ability of a desiccant solution to attract water vapour from

96　an air stream decreases with the increase of the solution temperature and the decrease of the

97　solution concentration [15]. In order to ensure dehumidifiers work with high efficiency and

98　minimise the carryover of desiccant droplets, internally cooled dehumidifiers which can allow

99　the desiccant solution working in a low temperature and low flow rate condition were studied

100　[16]. The performance comparison of an adiabatic dehumidifier with an internally cooled

101　dehumidifier showed that the dehumidification effectiveness of the internally cooled

102　dehumidifier was improved from 0.3876 - 0.4771 to 0.4769 - 0.7058, in comparison to that of

103　the adiabatic dehumidifier [17]. However, the inherent complex configuration of the internally

104　cooled dehumidifiers and high maintenance costs make these systems less attractive.

105　　Phase change materials (PCMs) with an ability to provide high energy storage densities and

106 the characteristics to store thermal energy at relatively constant temperatures have attracted

107 wide attention for developing high-performance buildings [18, 19]. The development of PCMs

108 and PCM thermal energy storage for liquid desiccant cooling systems have been reported in a

109 few studies [20-22]. Niu et al. [20], for instance, proposed to use micro-nanoencapsulated

110 PCMs as a heat transfer fluid to improve the performance of internally cooled dehumidifiers in

111 liquid desiccant cooling systems. The micro-nanoencapsulated PCMs were prepared and their

112 thermo-physical properties were characterised. However, the real application of such materials

113 in dehumidifiers was not reported. Al-Abidi et al. [21] and Mahdi and Nsofor [22] respectively

114 developed a triplex tube PCM thermal energy storage for liquid desiccant cooling systems. Al-

115 Abidi et al. [21] experimentally tested the charging performance of the PCM thermal storage

116 unit using a paraffin wax with a melting temperature of 82 ℃ while Mahdi and Nsofor [22]

117 numerically investigated the charging performance of the thermal energy storage using the same

118 paraffin wax but was enhanced by alumina nanoparticles and a porous copper foam. However,

119 both studies did not integrate the PCM thermal energy storage into liquid desiccant cooling

120 systems.

121   In this study, a novel phase change enhanced LiCl (i.e. PCM-LiCl) desiccant solution was

122 proposed to improve the dehumidification efficiency of adiabatic dehumidifiers. The new

123 solution was prepared by dispersing micro-encapsulated PCMs (MPCMs) into LiCl desiccant

124 solutions. As MPCMs have a relatively large thermal storage capacity, the dispersion of

125 MPCMs into liquid desiccant solutions can ensure the mixture work under a low temperature

126 condition, improving overall dehumidification efficiency. The properties of the new PCM-LiCl

127 desiccant solution such as density, enthalpy-temperature (h-T) relationship, particle size

128 distribution, thermal conductivity, and vapour pressure were characterised through either

129 experimental measurements or theoretical investigation.

130 **2. Development and characterisation of PCM-LiCl desiccant solutions**

131   Dehumidifiers can generally offer a better performance when the desiccant solution is

132 working in a low temperature condition such as in the range of 20-30 ℃ [23-24]. As shown in

133 Fig. 1a [25], the temperature of the LiCl desiccant solution is continuously increased along the

134 height of the adiabatic dehumidifier due to the heat and mass transfer between the process air

135 and the liquid desiccant and the absorption heat released during the dehumidification process.

136 This increased temperature will lead to the increase in the vapour pressure of the liquid

137 desiccant and therefore decrease the vapour pressure difference between the process air and

138 liquid desiccant, which deteriorates the moisture transfer and dehumidification effectiveness of

139 the adiabatic dehumidifier. This deterioration can be further confirmed by the results (see Fig.

140 1b) reported in another study [26], in which it was shown that the mass flux of moisture between

141 the process air and liquid desiccant decreased along the flow direction of the liquid desiccant.

142 As PCMs have a large storage density, the dispersion of MPCMs into liquid desiccants can

143 improve the thermal capacity of the mixture and therefore can decrease the temperature increase

144 of the liquid desiccant along the flow direction of the adiabatic dehumidifier, improving overall

145 dehumidification effectiveness.
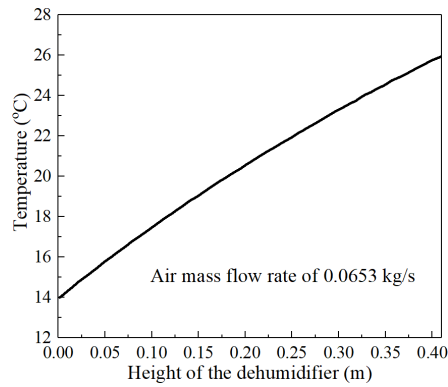
146

147 a) Temperature of the liquid desiccant [25]
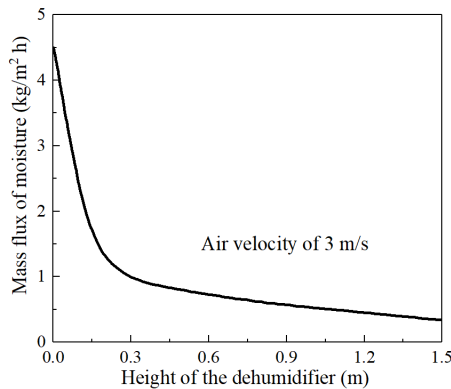
148

149 b) Mass flux of moisture [26]

150 Fig. 1. Temperature of LiCl liquid desiccant and mass flux of moisture along the flow

151 direction of an adiabatic dehumidifier.

152 In this study, two commercially available MPCM products, i.e. BASF Micronal DS 5038X

153 and Micronal DS 5040X with a melting temperature of 25 °C and 23 °C respectively, were used

154 to prepare phase change enhanced LiCl desiccant solutions. Both MPCMs were made of a

155 highly crosslinked polymethylmethacrylate (PMMA) polymer wall and paraffin inside as the

156 PCM. It is noted that the MPCMs used in this study might not be optimal. As the temperature

157 of the inlet working solution of the dehumidifier is a controlled variable, the phase change

158 materials should be selected based on the set-point of the inlet working solution temperature in

159 order to ensure that the PCM undergoes the phase change process during the dehumidification.

160 Deionized water and LiCl with a purity higher than 98% were used to prepare LiCl desiccant

161 solutions. The PCM-LiCl desiccant solution was prepared through directly dispersing the

162 MPCM particles into the LiCl desiccant solution via mechanical stirring.

163 **2.1 Characterisation of PCM-LiCl desiccant solutions**

164 To understand the likely benefits of using this new working solution for air

165 dehumidification, the properties of the PCM-LiCl desiccant solutions, including density, h-T

166 relationship, particle size distribution, thermal conductivity, and vapour pressure should be first

167 characterised. In this study, these properties were characterised through either theoretical

168 analysis or experimental measurements.

169 2.1.1 Density

170 The density of the PCM-LiCl desiccant solution was determined based on the density of

171 each insoluble component of the mixture as the potential non-homogeneity of the new solution

172 might introduce errors in measurements of the mixture. As the PMMA has good resistance to

173 LiCl and is insoluble in LiCl desiccant solutions, the density of the PCM-LiCl desiccant

174 solution can be calculated using Eq. (1) [27], in which the density of the MPCM was measured

175 using a pycnometer (to be introduced in Section 2.2) and the density of the LiCl desiccant

176 solution was determined using the correlation expressed in Eq. (2) [28].

177 $$\rho_{PCM\text{-}LiCl} = \frac{\rho_{PCM}\rho_{LiCl}}{\rho_{PCM}(1-x_{m,PCM})+\rho_{LiCl}x_{m,PCM}} \tag{1}$$

178 $$\rho_{LiCl} = \rho_{H2O}\sum_{i=0}^{3}\alpha_i\left(\frac{x_{m,LiCl}}{1-x_{m,LiCl}}\right)^i \tag{2}$$

179 where ρ is the density, α_i are the parameters and the values of α_0–α_3 were 1.0, 0.540966, -

180 0.303792, 0.100791, respectively [28], x_m is the mass fraction, and the subscripts *PCM-LiCl*,

181   *PCM* and *LiCl* indicate phase change enhanced LiCl desiccant solution, micro-encapsulated

182   phase change material, and LiCl desiccant solution, respectively.

183   2.1.2 Enthalpy-temperature (*h-T*) relationship

184   Differential scanning calorimeter (DSC) tests are commonly used to measure *h-T*

185   relationships of PCMs. In this study, the *h-T* relationship of the PCM-LiCl desiccant solution

186   was not measured directly as LiCl desiccant solutions may corrode the metal container of the

187   DSC device and further damage the equipment. Thus, the *h-T* relationship of the new solution

188   was determined using Eq. (3), based on the enthalpy of the LiCl desiccant solution determined

189   using Eq. (4) [29] and the DSC test results of the MPCMs.

190   $h_{PCM-LiCl}=x_{m,PCM} \, h_{PCM}+(1-x_{m,PCM}) \, h_{LiCl}$ (3)

191   $h_{LiCl}=A+BT+CT^2$ (4)

192   where h is the enthalpy, T is the temperature, and the coefficients of A, B, and C are calculated

193   using Eqs. (5-7) [29], respectively.

194   $A=-66.2324+11.2711x_{m,LiCl}-0.79853x^2_{m,LiCl}+(2.1534E-02)x^3_{m,LiCl}-(1.66352E-04)x^4_{m,LiCl}$

195   (5)

196   $B=4.5751-0.146924x_{m,LiCl}+(6.307226E-03)x^2_{m,LiCl}-$

197   $(1.38054E-04)x^3_{m,LiCl}+(1.06690E-06)x^4_{m,LiCl}$ (6)

198   $C=(-8.09689E-04)+(2.18145E-04)x_{m,LiCl}-(1.36194E-05)x^2_{m,LiCl}+(3.20998E-07)x^3_{m,LiCl}-$

199   $(2.64266E-09)x^4_{m,LiCl}$ (7)

200   2.1.3 Thermal conductivity

201   The thermal conductivity of the PCM-LiCl desiccant solution was calculated using

202 Maxwell's equation as shown in Eq. (8), which has been widely used to calculate the thermal

203 conductivity of MPCM suspensions [27, 30]. The thermal conductivity of the MPCM particles

204 (k_{PCM}) was determined using the composite sphere approach reported by Goel et al. [30], in

205 which the heat transfer resistance of the shell material was determined based on the thickness

206 of the MPCM shell. The heat transfer resistance of the core material was evaluated based on

207 the assumption that a solid sphere is in an infinite medium [31]. The thermal conductivity of

208 the MPCM can then be calculated using Eq. (9) [30]. The diameter of the MPCM particle was

209 measured using a particle size analyser to be introduced in Section 2.2 and the thickness of the

210 PMMA shell was determined using the composition of the MPCM measured using a

211 thermogravimetric analyser (see Section 2.2). The thermal conductivity of the LiCl desiccant

212 solution is calculated using Eq. (10) [28].

213 $$\frac{k_{PCM\text{-}LiCl}}{k_{LiCl}} = \frac{2k_{LiCl}+k_{PCM}+2x_{v,PCM}(k_{PCM}-k_{LiCl})}{2k_{LiCl}+k_{PCM}-x_{v,PCM}(k_{PCM}-k_{LiCl})} \qquad (8)$$

214 $$\frac{1}{k_{PCM}d_{PCM}} = \frac{1}{k_c d_c} + \frac{d_{PCM}-d_c}{k_s d_{PCM} d_c} \qquad (9)$$

215 $$k_{LiCl}=k_{H2O} - \alpha_R\, x_{m,LiCl,e} \qquad (10)$$

216 where k is the thermal conductivity, x_v is the volume fraction, d is the diameter, α_R is the

217 equivalent thermal conductivity depression, $x_{m,LiCl,e}$ is the equivalent ionic concentration, and

218 the subscripts s and c indicate shell and core, respectively.

219 2.1.4 Vapour pressure

220 The dehumidification performance of a liquid desiccant is directly influenced by the vapour

221 pressure difference between the liquid desiccant and process air [5]. In this study, the vapour

222 pressure of the PCM-LiCl desiccant solution was measured using a thermogravimetric method

223   [32]. In this method, the mass loss of the sample is measured using a thermogravimetric

224   analyser (i.e. TGA 5500 from TA Instruments was used in this study) and the result is then used

225   to determine the vapour pressure of the solution by using the Langmuir equation for free

226   vaporisation, as shown in Eq. (11) [33].

227    $log(P_T) = \beta_1 \, log\left(\frac{1}{\beta_2}\left|\frac{dm}{dt}\right|_T\right) + \beta_3$ (11)

228   where $\left|\frac{dm}{dt}\right|_T$ and P_T are the mass loss rate and the vapour pressure at a given temperature

229   respectively, and β_1, β_2 and β_3 are the coefficients influenced by the geometry structure of the

230   crucible. In this study, these three coefficients were determined based on the experimental

231   results for a reference substance (i.e. pure water) with the known vapour pressure.

232   During the test, the sample was placed in a sealed crucible with a 0.35 mm-diameter hole

233   on the lid, as illustrated in Fig. 2a. The crucible was then placed on the holder of the balance

234   inside the thermogravimetric analyser (Fig. 2b). The sample was purged by a pure nitrogen gas

235   flow in order to maintain the water content outside the crucible close to zero.

236
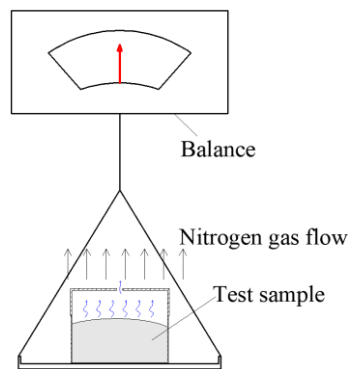
237

238   a) Schematic of vapour pressure measurement

239

240   b) Thermogravimetric analyser used in this study

241   **Fig. 2.** Vapour pressure measurement using a thermogravimetric analyser.

2.2 Characterisation of MPCMs and pure LiCl desiccant solutions

243   The properties of the MPCMs were determined either using the information provided in

244   the product data sheet [34] or through the experimental measurements.

245   The MPCM used was in a physical form of powder and the bulk density of the MPCM was

246   provided in the datasheet [34]. However, the particle density of the MPCM was required to

247   determine the density of the PCM-LiCl desiccant solutions. In this study, a pycnometer was

248   used to measure the particle density of the MPCM.

249   DSC tests were carried out to characterise the *h-T* relationship of the two MPCMs. The

250   tests were implemented using a micro DSC (micro DSC III, SETARAM) device with a weight

251   of the samples of around 300 mg. The heating/cooling rate used was 0.05 K/min.

252   The particle size distribution of the MPCM was measured using a laser diffraction particle

253   size analyser and the sample was pre-processed in an ultrasonic bath for deagglomeration of

254   the particles before the measurement. The results were analyzed using Mie model [35], which

255   worked well for homogeneous and spherical particles with a diameter less than 30 μm [36, 37].

256   The Mie model was derived by solving Maxwell's equations describing electromagnetic

257 radiation for the light scattered by a homogeneous sphere under the uniform illumination [35].

258 Thermogravimetric analysis was carried out using a thermogravimetric analyser to

259 determine the composition of the MPCMs, and then to calculate the thickness of the PMMA

260 shell. During the test, the MPCM was heated to a temperature of 600 $^\circ$C with a scanning rate of

261 1.0 K/min, and the test was then carried out using a nitrogen gas flow.

262 As LiCl is highly hygroscopic and pure LiCl may absorb the moisture from the air during

263 the preparation. A thermogravimetric analysis test for LiCl desiccant solutions was therefore

264 carried out to determine the mass fraction of LiCl in the solution. During the measurement, the

265 LiCl desiccant solution was heated to a temperature of 350 $^\circ$C with a scanning rate of 5.0 K/min

266 and was then maintained at 350 $^\circ$C for 18 hours [38]. The thermogravimetric analysis test was

267 also performed with a nitrogen gas flow.

268 **3. Results of properties characterisation**

269 In this section, the properties of the MPCMs and PCM-LiCl desiccant solutions were

270 respectively characterised using the methods introduced in Section 2. The majority of the tests

271 presented in this study were repeated in order to confirm the consistency of the results.

272 **3.1 Results of characterisation of MPCM properties**

273 The measured densities of the MPCM DS 5038X and MPCM DS 5040X were 990.9 $\pm$ 0.6

274 kg/m^3 and 1012.6 $\pm$ 0.4 kg/m^3, respectively. These results were considered to be reasonable as

275 the density of the two major compositions, i.e. paraffin wax and PMMA, were around 850 kg

276 m^{-3} and 1150 kg m^{-3}, respectively.

277 The DSC curves of the MPCM DS 5038X and MPCM DS 5040X are presented in Fig. 3

278 and their onset temperatures, peak temperatures, and heat of fusion during the cooling and

279 heating processes are summarized in Table 1. The heat of fusion of the MPCM was calculated

280 based on the temperature range of 15-28 °C. It can be observed that the peak phase change

281 temperatures of the MPCM DS 5038X for both heating and cooling were slightly higher than

282 those of the MPCM DS 5040X. The results from Table 1 also showed that the onset

283 temperatures of the MPCM DS 5038X were higher than those of the MPCM DS 5040X during

284 both cooling and heating processes.

285 **Table 1.** Onset temperatures, peak temperatures, and heat of fusion of the two MPCMs.

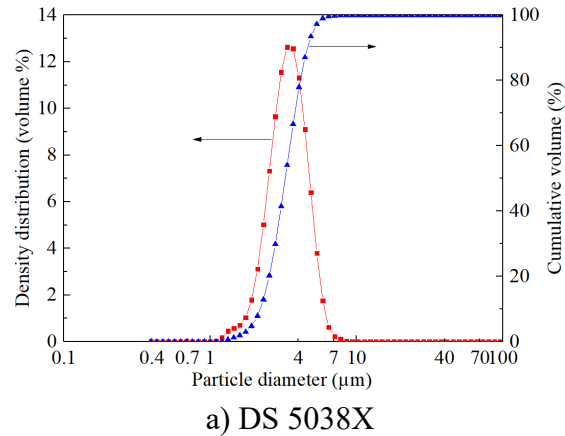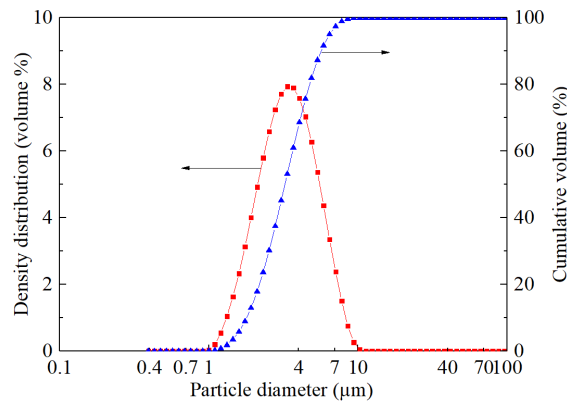|	DS 5038X			DS 5040X		
	Onset Temp. (°C)	Peak Temp.(°C)	Heat of fusion (J/g)	Onset Temp. (°C)	Peak Temp. (°C)	Heat of fusion (J/g)
Heating	22.55	25.37	96.7	19.87	24.64	94.8
Cooling	24.37	22.60	96.2	23.83	21.53	93.2

286
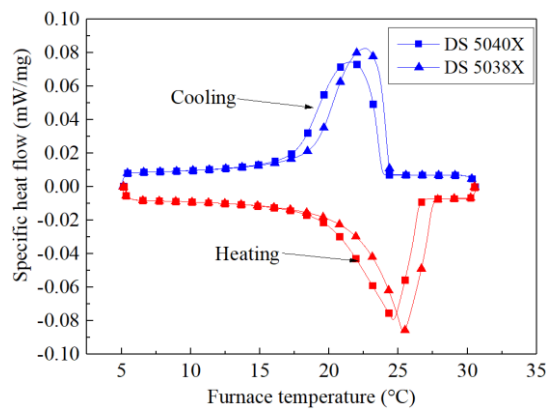
288 **Fig. 3.** DSC test results of DS 5038X and DS 5040X.

289 The measured particle size distributions of the MPCMs are presented in Fig. 4. The

290 volumetric average diameters of the MPCMs DS 5038X and DS 5040X were determined as

291 3.51 μm and 3.68 μm, respectively. It can be observed that the particle size distributions of both

292 MPCMs were in the range of 1 - 10 μm.

a) DS 5038X

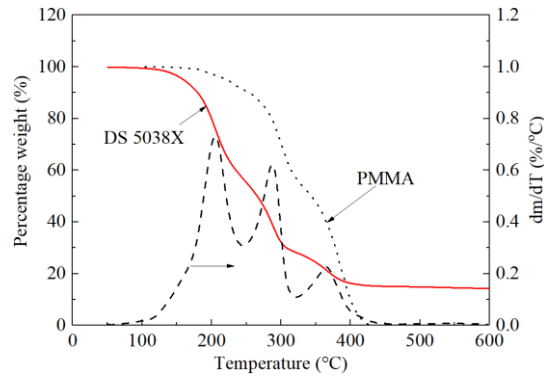b) DS 5040X

Fig. 4. Particle size distribution of the two MPCMs.

The results (i.e. percentage weight and mass loss rate of the sample) from the thermogravimetric analysis of the MPCMs DS 5038X and DS 5040X and a sample of the MPCM DS 5038X after the decomposition test are presented in Fig. 5. The thermogravimetric analysis results of the shell material (i.e. PMMA) obtained from [39] were also provided. It can be seen that the thermal degradation of the MPCM DS 5038X can be divided into three phases and the MPCM was mainly decomposed in the first two phases at a temperature below 330 ℃, and the PMMA was completely decomposed at a temperature of around 454 ℃ (Fig. 5a). Similar trends were also observed for the MPCM DS 5040X (Fig. 5b). By comparing the thermogravimetric analysis curve of the MPCM to that of the PMMA, it can be derived that the

307   composition of the MPCM DS 5038X was 17.4% wt. PMMA, 67.5% wt. paraffin, and 15.1%

308   wt. residual and that of the MPCM DS 5040X was 17.1% wt. PMMA, 69.5% wt. paraffin, and

309   13.4% wt. residual. The similar results were also reported in [37, 40].

310

311
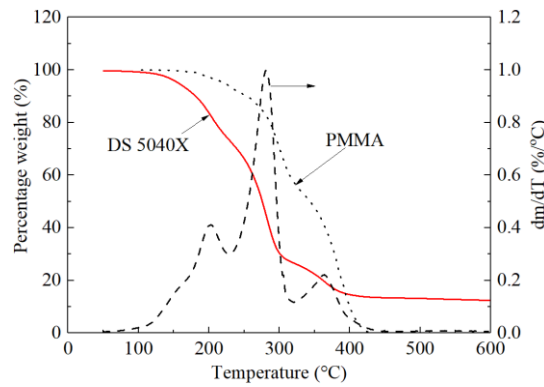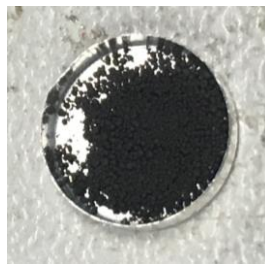312   a) DS 5038X

313

314   b) DS 5040X

315
316   c) DS 5038X after the decomposition test

317   **Fig. 5.** Decomposition of PMMA [39], MPCM DS 5038X and MPCM DS 5040X.

318   **3.2 Results of characterisation of PCM-LiCl desiccant solutions**

319   3.2.1 Verification of vapour pressure measurement

320   The vapour pressure of the LiCl desiccant solution was measured using the

17

321 thermogravimetric method and the results were compared with the calculated values determined

322 using the correlation expressed in Eq. (12) [28]. The concentration of the LiCl desiccant

323 solution was first determined via a thermogravimetric analysis test and the vapour pressure of

324 the LiCl desiccant solution was then measured at a temperature of 50 $^{\circ}$C using the method

325 presented in Fig. 2. The test results are presented in Fig. 6, which were measured based on the

326 initial concentration of the LiCl solution of 29.53%. It can be found that the vapour pressure of

327 the solution decreased with the increase of the solution concentration and the measured values

328 generally agreed well with the calculated results. The average and maximum deviations

329 between the measured and calculated values were 1.9% and 5.5%, respectively. It is worthwhile

330 to note that the total mass of the test sample used was relatively small due to the capacity of the

331 crucible used and the increase of the concentration was resulted by the continuous loss of the
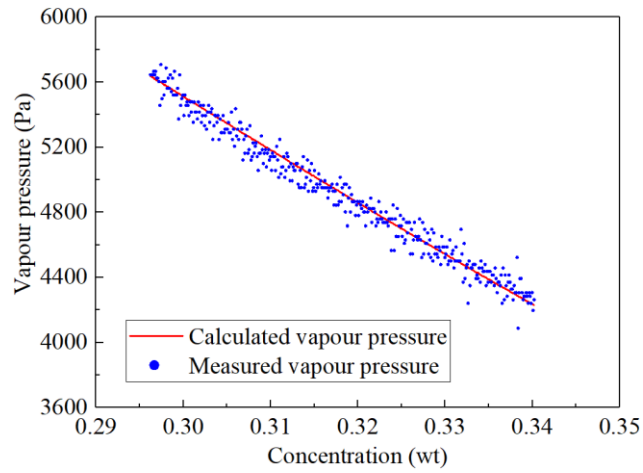
332 water in the solution.

333 $P_{LiCl}=\pi_{25}f(x_{m,LiCl},\theta)P_{H2O}$ (12)

334 where θ is the reduced temperature, $f(x_{m,LiCl},\ \theta)$ is determined using Eq. (13) [28], and π_{25} is

335 calculated using Eq. (14) [28].

336 $f(x_{m,LiCl},\theta)=2-[1+(\frac{x_{m,LiCl}}{\pi_0})^{\pi_1}]^{\pi_2}+\{[1+(\frac{x_{m,LiCl}}{\pi_3})^{\pi_4}]^{\pi_5}-1\}\theta$ (13)

337 $\pi_{25}=1-[1+(\frac{x_{m,LiCl}}{\pi_6})^{\pi_7}]^{\pi_8}-\pi_9 exp(-\frac{(x_{m,LiCl}-0.1)^2}{0.005})$ (14)

338 where π_0-π_8 are the coefficients and the values used were provided in Table 2 [28].

Fig. 6. Measured and calculated vapour pressures of the LiCl desiccant solution.

**Table 2.** Coefficients for vapour pressure calculation of LiCl desiccant solutions [28].

π_0	π_1	π_2	π_3	π_4	π_5	π_6	π_7	π_8	π_9
0.28	4.30	0.60	0.21	5.10	0.49	0.362	-4.75	-0.40	0.03

3.2.2 Properties characterisation

In this study, the LiCl desiccant solution with a concentration of 35% was first prepared and the MPCMs with different mass fractions were then mixed with the LiCl desiccant solution to prepare the PCM-LiCl desiccant solutions. The densities of different PCM-LiCl desiccant solutions were then calculated using Eqs. (1) and (2) and the results are presented in Fig. 7. It can be seen that the density of the PCM-LiCl desiccant solutions decreased with the increase of the mass fraction of the MPCMs as the density of the MPCMs was lower than that of the LiCl desiccant solution. The density of the mixture using the MPCM DS 5038X was always lower than that using the MPCM DS 5040X which was resulted by the relatively low density of the MPCM DS 5038X. It is noted that the density of the mixture calculated using Eq. (1) [27]

19

354   is applicable to homogenous fluids and the PCM-LiCl desiccant solution developed in this study

355   can be considered as homogenous when it is well mixed.
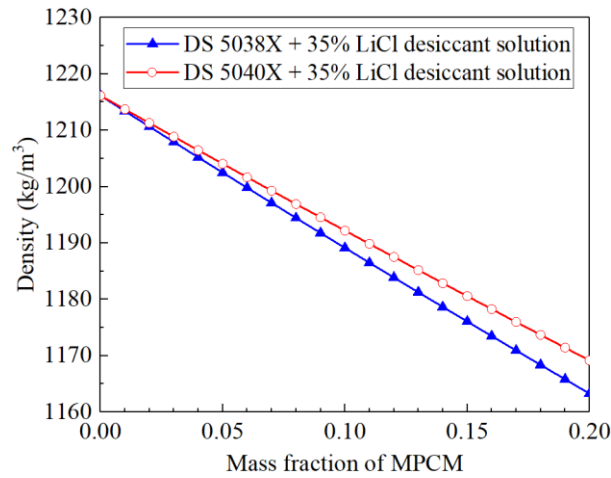
356

357   **Fig. 7.** Density of the PCM-LiCl desiccant solution.

358   The *h-T* relationship of the PCM-LiCl desiccant solutions was determined using Eqs. (3)

359   and (4). The heating curve of the MPCM obtained from the DSC measurement was used to

360   evaluate the enthalpy of the MPCM. The results are presented in Fig. 8. The enthalpy of the

361   LiCl desiccant solution without MPCMs was also presented in this figure. It can be observed

362   that the enthalpy of the PCM-LiCl desiccant solution increased with the increase of the solution

363   temperature and the mass fraction of the MPCMs in the mixture. A large increasing rate
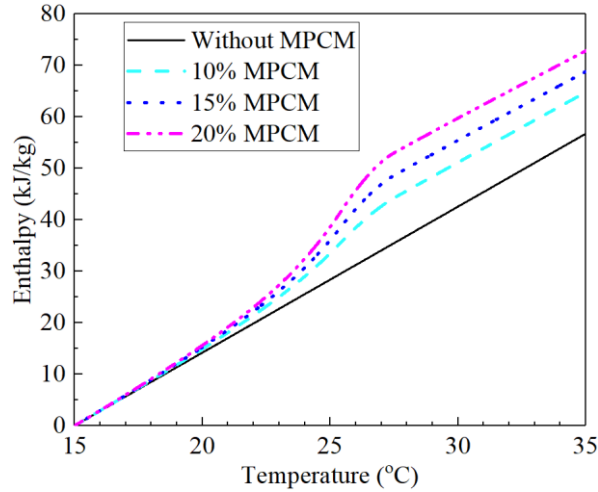
364   occurred in the MPCM melting temperature range of 20-27 °C. The enthalpy of the solution

365   then increased almost linearly if further increasing the solution temperature. There was not a
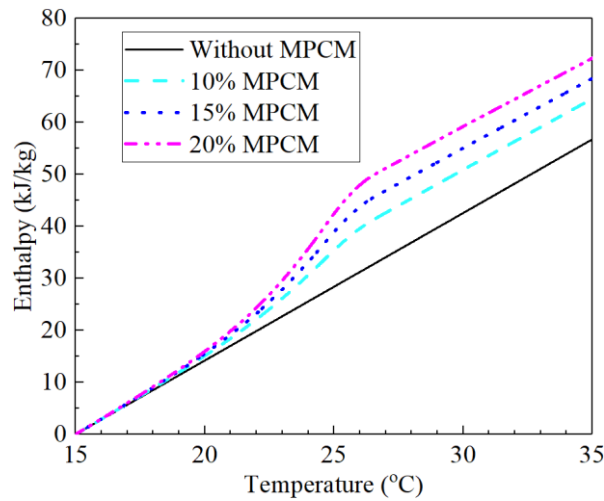
366   clear difference between the use of two different MPCMs.

a) DS 5038X

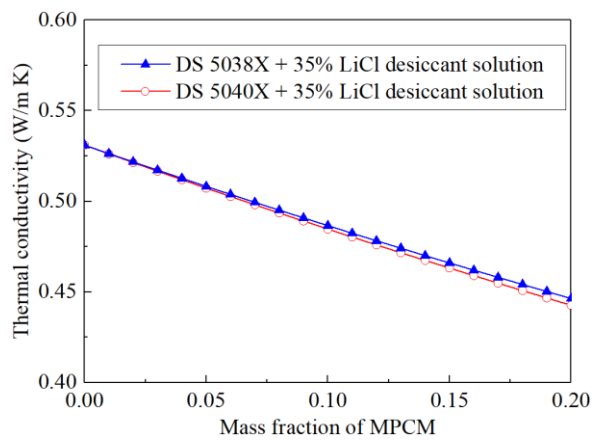b) DS 5040X

Fig. 8. Enthalpy-temperature relationships of the pure LiCl desiccant solution and PCM-LiCl

desiccant solutions with different mass fractions of the MPCMs.

The thermal conductivity of the PCM-LiCl desiccant solution was calculated using Eqs. (8)

and (9) based on the composition and particle size of the MPCM determined. It is noted that

the diameter of the particles dispersed into the LiCl desiccant solution was assumed to be the

same as the volumetric average diameter of the particles. It was also assumed that the residual

of the MPCMs obtained from the thermogravimetric analysis had the same thermal conductivity

378   as the PCM used. The resulted thermal conductivity of the PCM-LiCl desiccant solutions is

379   presented in Fig. 9. It can be observed that the thermal conductivities of the PCM-LiCl desiccant

380   solutions using the MPCM DS 5040X and DS 5038X were very close to each other when the

381   mass fraction of the MPCMs was less than 20%. The thermal conductivity of the PCM-LiCl

382   desiccant solutions decreased with the increase of the mass fraction of the MPCMs as the

383   thermal conductivity of the MPCM particle was lower than that of the LiCl desiccant solution.

384

385   **Fig. 9.** Thermal conductivity of the PCM-LiCl desiccant solutions with different mass

386   fractions of MPCMs.

387   The vapour pressures of the PCM-LiCl desiccant solutions with different mass fractions of

388   the two MPCMs were measured using the thermogravimetric method. As the variation in the

389   vapour pressures of the PCM-LiCl solutions using the two MPCMs showed a similar trend, the

390   results of the PCM-LiCl solution using the MPCM DS 5040X under the temperature of 50 °C

391   were presented only.

392   During the measurement, the LiCl desiccant solution was first prepared and the

393   concentration of the LiCl desiccant solution was determined via a thermogravimetric analysis

394   test. A relatively low initial concentration of the LiCl desiccant solution (i.e. 29.53%) was used

395   to prepare PCM-LiCl desiccant solutions as the concentration of the desiccant solution was

396   expected to increase during the vapour pressure measurement due to continuous loss of the

397   water in the solution. The PCM-LiCl desiccant solution was then prepared in the crucible

398   presented in Fig. 2a. Table 3 summarises the details of the three samples used in the test. It is

399   worthwhile to note that the mass fraction of the MPCM in each test sample cannot be precisely

400   controlled during the preparation.

401

402   **Table 3.** Test samples prepared for vapour pressure measurement.

Test sample	Weight (mg)	Mass fraction of the MPCM	Mass fraction of the LiCl
Sample 1	49.158	0.029	0.288
Sample 2	57.424	0.128	0.258
Sample 3	54.190	0.180	0.243

403

404   The measurement results of the PCM-LiCl desiccant solution using the MPCM DS 5040X

405   under the temperature of 50 °C are presented in Figs. 10 and 11. The vapour pressures of LiCl

406   desiccant solutions without the MPCM were also presented, which were calculated based on

407   the same temperature condition and the same initial mass fractions of LiCl in the desiccant

408   solutions as those presented in Table 3. The vapour pressure of the pure LiCl desiccant solution

409   was determined using Eqs. (12)-(14). It can be seen that the vapour pressures of the PCM-LiCl

410   desiccant solutions of three samples continuously decreased as a function of time. This is

411   because the mass fractions of both MPCM and LiCl continuously increased with time during

412   the test due to the water loss (Fig. 11). For each test sample, the vapour pressure of the PCM-

413   LiCl desiccant solution was always lower than that of the pure LiCl desiccant solution during

414   the test period due to the existence of the MPCM particles. The vapour pressure of the PCM-

415   LiCl desiccant solution decreased with the increase of the mass fraction of the MPCM in the

416   mixture.
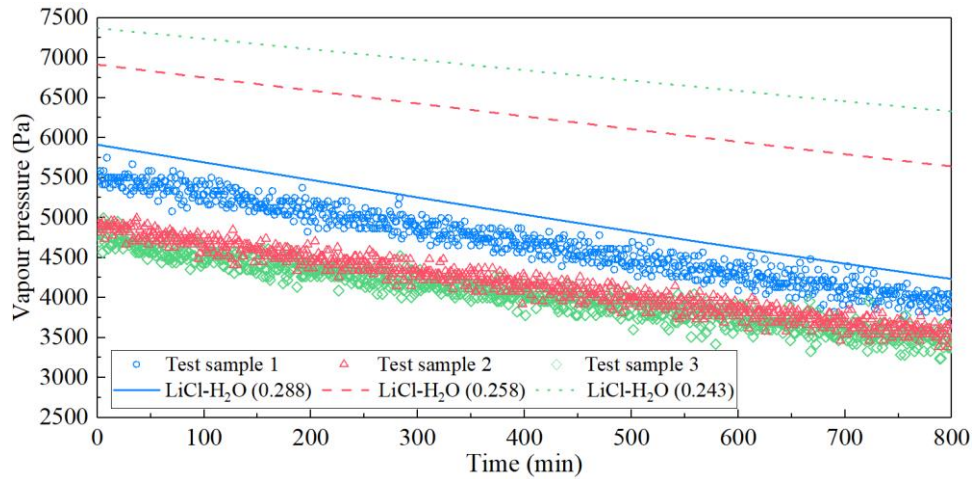
417

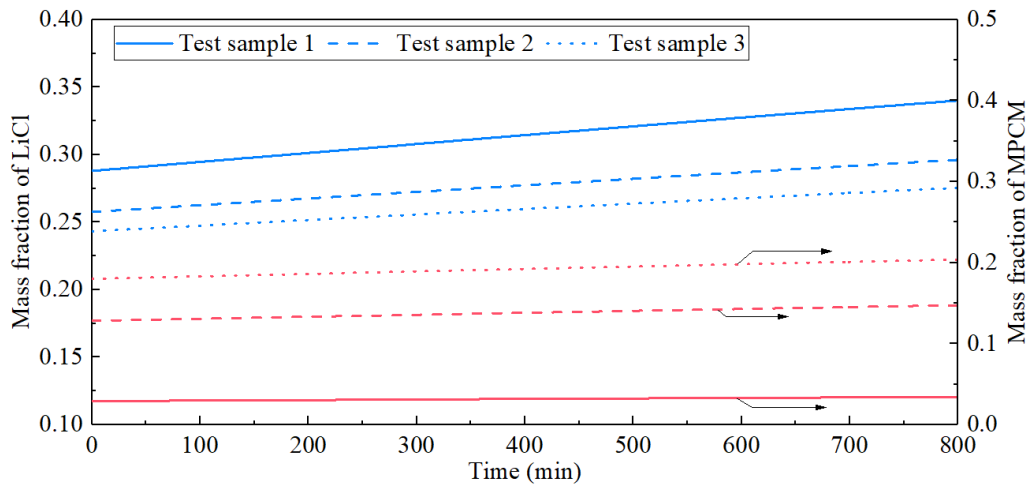418   **Fig. 10.** Variation of vapour pressure of the PCM-LiCl desiccant solutions and pure LiCl

419   desiccant solutions as a function of time.

420

421   **Fig. 11.** Variation of mass fractions of the MPCM and LiCl in the PCM-LiCl desiccant

422   solutions as a function of time.

423

424   From the above results, it can be concluded that the dispersion of MPCMs into the liquid

425 desiccant solution can decrease the vapour pressure and increase the thermal capacity of the

426 mixture, which can improve the dehumidification efficiency of adiabatic dehumidifiers

427 although the thermal conductivity of the mixture was slightly decreased. In principle, a low

428 solution flow rate can be used in the liquid desiccant cooling system when using the PCM-LiCl

429 desiccant solution due to the increased thermal capacity and reduced vapour pressure. It is also

430 expected that the size of the dehumidifier using the new working solution can be decreased

431 without compromising the dehumidification performance, when compared to the dehumidifier

432 using pure desiccant solutions. In addition, the temperature of the inlet solution to the

433 dehumidifier should be optimised in order to maximise the benefits of using MPCMs in the

434 desiccant solution. It is also noteworthy that thermal regeneration might not be an optimal

435 method for liquid desiccant cooling systems when using PCM-LiCl desiccant solutions and

436 non-thermal regeneration methods may be required, which will be investigated in future studies.

437 However, the potential benefits of using PCM-LiCl desiccant solutions should be evaluated in

438 liquid desiccant cooling systems by considering the influence of the MPCM particles in both

439 dehumidifiers and regenerators. Adding the MPCM particles into liquid desiccant solutions

440 may increase the power consumptions of the circulation pump. Meanwhile, the mass fraction

441 of the MPCMs in the mixture should be optimised. The long-term performance and potential

442 segregation of MPCM particles in the new working solution should also be examined.

443 **4. Conclusions**

444   This study presented the development and characterisation of a new phase change enhanced

445 working solution for liquid desiccant cooling systems. The new solution was prepared through

446 dispersion of micro-encapsulated PCMs (i.e. Micronal DS 5038X and DS 5040X) into the base

447 fluid of the LiCl desiccant solution. The properties including density, *h-T* relationship, thermal

448 conductivity, particle size distribution, and vapour pressure of the new solution were

449 characterised either through direct measurement or theoretical analysis.

450 The results showed that the density of the phase change enhanced LiCl (PCM-LiCl)

451 desiccant solution decreased with the increase of the mass fraction of the MPCMs in the mixture

452 due to the lower density of the MPCMs used in comparison with the pure LiCl solutions. The

453 thermal capacity of the PCM-LiCl desiccant solutions was substantially increased in the melting

454 range of the MPCMs. The thermal conductivities of the PCM-LiCl desiccant solutions using

455 the MPCMs DS 5038X and DS 5040X were very close to each other when the mass fraction of

456 the MPCMs was less than 20% and the thermal conductivity decreased with the increase of the

457 mass fraction of the MPCMs. The vapour pressure of the new working solution decreased due

458 to the existence of the MPCM particle as compared to the LiCl solution without using the

459 MPCMs. The dehumidification performance of adiabatic dehumidifiers could be potentially

460 improved by using this new working solution due to its decreased vapour pressure and increased

461 thermal capacity, which will be investigated in our future studies.

462 **Acknowledgement**

466 **References**

467 [1] P.G. Dixon, M. Sinyor, A. Schaffer, A. Levitt, C.R Haney, K.N Ellis, S.C Sheridan,

468 Association of weekly suicide rates with temperature anomalies in two different climate types,

469 International Journal of Environmental Research and Public Health 11 (11) (2014) 11627-11644.

470 [2] H. Chappells, E. Shove, Debating the future of comfort: environmental sustainability,

471 energy consumption and the indoor environment, Building Research & Information 33 (1)

472 (2005) 32-40.

473 [3] R.C. Arora, Refrigeration and air conditioning, PHI Learning Pvt. Ltd., New Delhi, 2012.

474 [4] American Society of Heating, Refrigerating and Air-Conditioning Engineers (ASHRAE),

475 ASHRAE Handbook-Fundamentals, ASHRAE, Atlanta, 2009.

476 [5] L. Mei, Y.J. Dai, A technical review on use of liquid-desiccant dehumidification for air-

477 conditioning application, Renewable and Sustainable Energy Reviews 12 (3) (2008) 662-689.

478 [6] A.H. Abdel-Salam, C.J Simonson, State-of-the-art in liquid desiccant air conditioning

479 equipment and systems, Renewable and Sustainable Energy Reviews 58 (2016) 1152-1183.

480 [7] Y. Guo, Z. Ma, A. Al-Jubainawi, P. Cooper, L.D. Nghiem, Using electrodialysis for

481 regeneration of aqueous lithium chloride solution in liquid desiccant air conditioning systems,

482 Energy and Buildings 116 (2016) 285-295.

483 [8] D.L. Shukla, K.V. Modi, A technical review on regeneration of liquid desiccant using solar

484 energy, Renewable and Sustainable Energy Reviews 78 (2017) 517-529.

485 [9] S.W. Ham, S.J. Lee, J.W. Jeong, Operating energy savings in a liquid desiccant and dew

486 point evaporative cooling-assisted 100% outdoor air system, Energy and Buildings 116 (2016)

487 535-552.

488   [10]T. Elmer, M. Worall, S. Wu, S. Riffat, An experimental study of a novel integrated desiccant

489   air conditioning system for building applications, Energy and Buildings 111 (2016) 434-445.

490   [11]Y. Chen, H. Yang, Y. Luo, Investigation on solar assisted liquid desiccant dehumidifier and

491   evaporative cooling system for fresh air treatment, Energy 143 (2018) 114-127.

492   [12]L-DCS Technology, http://www.l-dcs.de/, 2018 (accessed 15 December 2018)

493   [13]A. Hublitz, Efficient Energy Storage in Liquid Desiccant Cooling Systems, Ph.D Thesis,

494   Technische Universität München, München, Germany, 2008.

495   [14]M.M. Rafique, P. Gandhidasan, H.M. Bahaidarah, Liquid desiccant materials and

496   dehumidifiers–A review, Renewable and Sustainable Energy Reviews 56 (2016) 179-195.

497   [15]N. Fumo, D.Y. Goswami, Study of an aqueous lithium chloride desiccant system: air

498   dehumidification and desiccant regeneration, Solar Energy 72 (4) (2002) 351-361.

499   [16]A. Lowenstein, Review of liquid desiccant technology for HVAC applications, HVAC&R

500   Research 14 (6) (2008) 819-839.

501   [17]P. Bansal, S. Jain, C. Moon, Performance comparison of an adiabatic and an internally

502   cooled structured packed-bed dehumidifier, Applied Thermal Engineering 31 (1) (2011) 14-19.

503   [18]Z. Ma, W. Lin, M.I. Sohel, Nano-enhanced phase change materials for improved building

504   performance, Renewable and Sustainable Energy Reviews 58 (2016) 1256-1268.

505   [19]Z. Hu, A. Li, R. Gao, H. Yin, A comparison study on melting inside the rectangular and

506   curved unit with a vertical heating wall, Journal of Thermal Analysis and Calorimetry 122 (2)

507   (2015) 831-842.

508   [20]X. Niu, Q. Xu, Y. Zhang, Y. Zhang, Y. Yan, T. Liu, Fabrication and properties of micro-

509 nanoencapsulated phase change materials for internally-cooled liquid desiccant

510 dehumidification, Nanomaterials 7 (5) (2017) 96.

511 [21]A.A. Al-Abidi, S. Mat, K. Sopian, M.Y. Sulaiman, A. T. Mohammad, Experimental study

512 of PCM melting in triplex tube thermal energy storage for liquid desiccant air conditioning

513 system, Energy and Buildings 60 (2013) 270-279.

514 [22]J.M. Mahdi, E.C. Nsofor, Melting enhancement in triplex-tube latent heat energy storage

515 system using nanoparticles-metal foam combination, Applied Energy 191 (2017) 22-34.

516 [23]L. Wang, F. Xiao, X. Zhang, R. Kumar, An experimental study on the dehumidification

517 performance of a counter flow liquid desiccant dehumidifier, International Journal of

518 Refrigeration 70 (2016) 289-301.

519 [24]X.H. Liu, Y. Jiang, K.Y. Qu, Heat and mass transfer model of cross flow liquid desiccant

520 air dehumidifier/regenerator, Energy Conversion and Management 48 (2) (2007) 546-554.

521 [25]I.P. Koronaki, R.I. Christodoulaki, V.D. Papaefthimiou, E.D. Rogdakis, Thermodynamic

522 analysis of a counter flow adiabatic dehumidifier with different liquid desiccant materials,

523 Applied Thermal Engineering 50 (1) (2013) 361-373.

524 [26]M.R. Islam, S.W.L. Alan, K.J. Chua, Studying the heat and mass transfer process of liquid

525 desiccant for dehumidification and cooling, Applied Energy 221 (2018) 334-347.

526 [27]B. Chen, X. Wang, R. Zeng, Y. Zhang, X. Wang, J. Niu, Y. Li, H. Di, An experimental study

527 of convective heat transfer with microencapsulated phase change material suspension: laminar

528 flow in a circular tube under constant heat flux, Experimental Thermal and Fluid Science 32 (8)

529 (2008) 1638-1646.

530   [28] M.R. Conde, Properties of aqueous solutions of lithium and calcium chlorides:

531   formulations for use in air conditioning equipment design, International Journal of Thermal

532   Sciences 43 (4) (2004) 367-382.

533   [29] S.K. Chaudhari, K.R Patil, Thermodynamic properties of aqueous solutions of lithium

534   chloride, Physics and Chemistry of Liquids 40 (3) (2002) 317-325.

535   [30] M. Goel, S.K. Roy, S. Sengupta, Laminar forced convection heat transfer in

536   microcapsulated phase change material suspensions, International Journal of Heat and Mass

537   Transfer 37 (4) (1994) 593-604.

538   [31] E.C. Guyer, Handbook of applied thermal design, CRC Press, Philadelphia, 1999.

539   [32] D.M. Price, Vapor pressure determination by thermogravimetry, Thermochimica Acta (367)

540   (2001) 253-262.

541   [33] S. Giani, Determination of vapor pressure and the enthalpy of vaporization by TGA,

542   METTLER TOLEDO Thermal Analysis UserCom 38 (2014) 15-18.

543   [34] Micronal Product Manual, https://www.microteklabs.com/micronal, 2018 (accessed 10

544   December 2018).

545   [35] D.L. Black, M.Q. McQuay, M.P. Bonin, Laser-based techniques for particle-size

546   measurement: a review of sizing methods and their industrial applications, Progress in Energy

547   and Combustion Science 22 (3) (1996) 267-306.

548   [36] G.B. de Boer, C. de Weerd, D. Thoenes, H.W. Goossens, Laser diffraction spectrometry:

549   Fraunhofer diffraction versus Mie scattering, Particle & Particle Systems Characterization 4 (1-

550   4) (1987) 14-19.

551   [37] J. Giro-Paloma, G. Oncins, C. Barreneche, M. Martínez, A.I. Fernández, L.F. Cabeza,

552   Physico-chemical and mechanical properties of microencapsulated phase change material,

553   Applied Energy 109 (2013) 441-448.

554   [38]P. Masset, Thermogravimetric study of the dehydration reaction of $LiCl \cdot H2O$, Journal of

555   Thermal Analysis and Calorimetry 96 (2) (2009) 439-441.

556   [39]M.C. Costache, D. Wang, M.J. Heidecker, E. Manias, C.A. Wilkie, The thermal degradation

557   of poly (methyl methacrylate) nanocomposites with montmorillonite, layered double

558   hydroxides and carbon nanotubes, Polymers for Advanced Technologies 17 (4) (2006) 272-280.

559   [40]J. Giro-Paloma, C. Barreneche, M. Delgado, M. Martínez, A.I. Fernández, L.F. Cabeza,

560   Physicochemical and thermal study of a MPCM of PMMA shell and paraffin wax as a core,

561   Energy Procedia 54 (2014) 347-354.